Scanning Electron Microscopy

Volume 4
Number 1 *The Science of Biological Specimen Preparation for Microscopy and Microanalysis*

Article 29

1985

The Morphology of Thin Metal Coatings Formed by Rotary Shadowing Biological Species in High Vacuum

J. A. Panitz
Sandia National Laboratories

Science of Biological Specimen Preparation (pp. 283-288)
SEM Inc., AMF O'Hare (Chicago), IL 60666-0507, U.S.A.

THE MORPHOLOGY OF THIN METAL COATINGS FORMED BY ROTARY SHADOWING BIOLOGICAL SPECIES IN HIGH VACUUM

J. A. Panitz

Sandia National Laboratories
Surface Science Division 1134
Albuquerque, NM 87185 (USA)
Phone: (505) 844-5457

Abstract

Rotary Shadowing has been used to increase the image contrast of biological species observed during edge-projection imaging in the transmission electron microscope. In this imaging mode, biological species are adsorbed from aqueous solutions onto a highly curved substrate and viewed, over its edge, in a direction parallel to its surface. Since the substrate is not placed between a biological adsorbate and the photographic emulsion that records its image, any material can be used as a support (including high-Z metals and semiconductors). Binding to these technologically interesting materials is observed with unusual clarity and contrast, even at 200kV. Individual adsorbates and multilayer structures are clearly delineated by a thin, metal shadow layer that surrounds them. As expected, gold and platinum form rough, discontinuous and coarse grained layers, while tungsten layers are smooth, continuous and fine grained on a subnanometer scale. Edge-projection imaging, in conjunction with rotary shadowing, is providing a unique view of shadow layer morphology, and the first images of protein molecules, virus particles, and multilayers formed by the immune reaction.

Key Words: Coating, Deposition, Edge-Projection, TEM, Protein, Field-Emitter, Layer, Metal, Morphology, Shadow, Tip.

Introduction

The transmission electron microscope (TEM) is a valuable tool for visualizing the shape of biological species. Unfortunately, image contrast is usually quite poor, even when species are placed on very thin support films and imaged at low incident electron energies. In order to increase the contrast of biological species they can be encapsulated into a "low noise" matrix (Muller et al., 1975), but are usually coated with a thin layer of a high-Z metal prior to TEM imaging. For example, the study of proteins, nucleic acids, and their interaction with each other has been greatly facilitated by observing these species in the TEM after coating them with tungsten (Fisher and Williams, 1979). The coating procedure (known as "rotary shadowing") is straightforward: A metal is evaporated at a low angle onto a support film on which a biological species has been deposited. The support film is slowly rotated during the evaporation process in order to obtain a very uniform coating of metal on the surface. Contrast in the resulting TEM image is generated by the different thicknesses of metal encountered by the incident electron beam as it penetrates an adsorbate (and the support film) on its way to a photographic emulsion. Image resolution depends upon the ability of the metal coating to faithfully replicate topological features of an adsorbate. For this reason, it is desirable to deposit very thin ($\sim$ 1nm thick), continuous metal films onto an adsorbate for shadowing purposes. Refractory metals are known to produce such coatings on room temperature substrates (Thornton, 1982; Chopra, 1969). High contrast TEM images of DNA, proteins, and nucleoprotein complexes are routinely obtained with about 1nm resolution after rotary shadowing with tungsten (Griffith and Christiansen, 1978).

This paper describes a new way to visualize biological species in the TEM after rotary shadowing. The images that are obtained are unusual in that they visualize an adsorbate in a direction parallel to a substrate -- a substrate that can be prepared from any material, including high-Z metals and semiconductors. We are using this approach to characterize the formation of immunologic multilayers on technologically interesting materials (Panitz, 1985a). The

successful development of new biomolecular devices (Carter, 1983) will depend on a knowledge of biomolecular adsorption on these materials. In this paper we will describe our "edge-projection" imaging and shadowing procedure (Panitz and Bear, 1985) in detail. We will confirm many of the previous TEM observations of rotary shadowed, coating morphology but without the contrast artifacts introduced by a supporting film.

Edge-Projection TEM

A TEM image of a biological species is usually formed by passing a focussed electron beam through the species and through a thin carbon or plastic film that provides support. Since the electron beam must pass through the supporting film, the contrast generated by the support will contribute to the contrast of the final image. The contrast generated by the support can introduce artifacts that can make image interpretation difficult (Lins, 1984). In order to minimize this problem, we used an alternate imaging geometry in which biological species were supported by a highly curved substrate positioned at right angles to the imaging direction (Panitz and Giaever, 1980). Since the supporting substrate is not positioned between the species and the photographic emulsion that recorded their image, a micrograph free of support-generated artifacts is produced. Unfortunately, image contrast was very marginal for all species except thick protein multilayers (produced by the immune reaction) or individual molecules like ferritin that contained a high concentration of a heavy metal (Panitz and Giaever, 1981). In order to extend the imaging technique to other biological species, we have increased the contrast by adapting an established method for obtaining high contrast, high resolution TEM images of nucleic acids by rotary shadowing them with tungsten in high vacuum (Griffith, 1973). Figure 1 is a schematic drawing of the geometry we use to produce an edge-projection, transmission electron microscope (EPTEM) image of a rotary shadowed, biological species. The trick is to obtain a highly curved substrate with a surface that is very smooth over molecular dimensions. Fortunately, a great deal is known about preparing smooth, highly curved substrates.

Field-emitter tips as substrates

The highly curved substrate that we use for EPTEM imaging is the apex of a slender, needle-like, field-emitter "tip". Metallic field-emitter tips were used more than fifty years ago to examine the phenomenon of "cold" or "Field-emission" of electrons in high vacuum (Eyring et al., 1928). Nine years later single field-emitter tips were being used as point sources of electrons in the field-electron emission microscope (Müller, 1937). Today, field-emitter tips are being used as bright, monochromatic, point sources of electrons for high resolution electron microscopy.

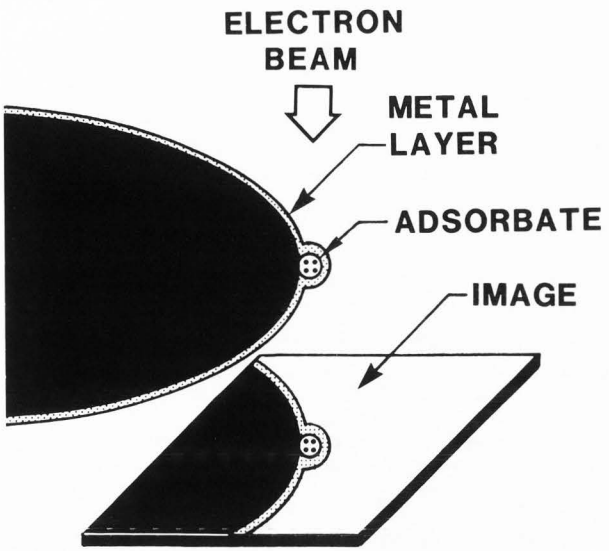

Figure 1. A schematic drawing of the Edge-Projection Transmission Electron Microscope (EPTEM) imaging process.

The apex radius of curvature of a typical field-emitter tip is about 200nm. A tip can be fabricated from almost any material including insulators, metals, and semiconductors (Müller and Tsong, 1969). Tungsten tips are probably the easiest to fabricate (Dyke and Dolan, 1960), and were obtained commercially for this study from the FEI Company (Hillsboro, Oregon). These tips were prepared by electrochemically polishing a polycrystalline tungsten rod in 1M NaOH at a few volts DC for several minutes. After polishing, the tips were cleaned by thermal annealing in high vacuum at 1800K for a few minutes. The annealing process produces a smooth, almost perfect hemispherical contour at the tip apex by surface self-diffusion (Boling and Dolan, 1958). Figure 2a is a low magnification image of a typical tip used in this study. Figure 2b shows the same tip mounted in an adapter that is positioned in the side entry goniometer stage of a commerical TEM prior to EPTEM imaging. The surface roughness of the tip apex is much less than 1nm as can be seen in the EPTEM image shown in Figure 3.

Rotary Shadowed Field-emitter tips

The shadowing geometry that we use is shown schematically in Figure 4. Although an evaporation angle of nine degrees is shown in the figure, any angle between about five and fifteen degrees works quite well. It is important to remember that the tip apex is highly curved so that the effective evaporation angle will change as a function of distance from the tip apex. Within our usual imaging area (about twenty degrees from the tip axis) the thickness and the morphology of the metal coating remains constant.

Metals with a low melting point (such as gold and platinum) are evaporated onto a tip from a

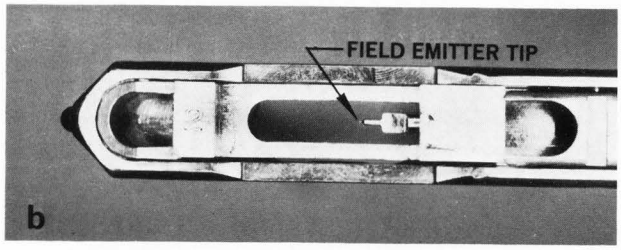

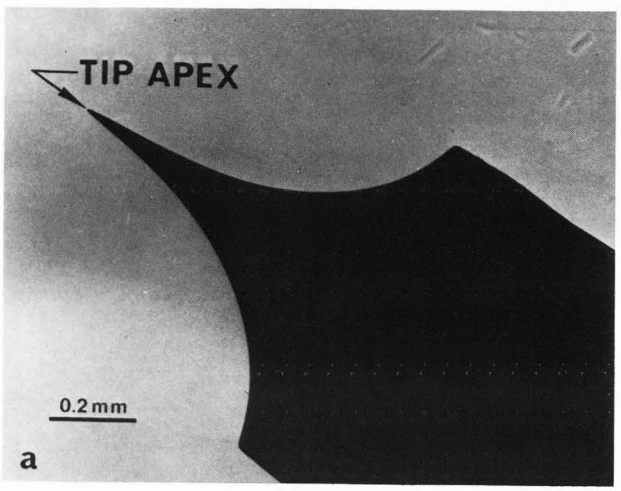

Figure 2. (a) A low magnification image of a tungsten field-emitter tip. (b) A field-emitter tip mounted in an adapter that has been placed in the side entry goniometer stage of a transmission electron microscope prior to EPTEM imaging.

tungsten filament by wetting the filament with the appropriate material and then raising the filament temperature just enough to evaporate the coating. High melting point materials (such as tungsten) are deposited by heating a filament of the appropriate material to incandescence. One to ten tips can be coated with metal at the same time by placing them in holes drilled into an aluminum block centered on a rotary table shown in Figure 4. The holes are equally spaced along the perimeter of a circle about 8 mm in diameter. Each tip is adjusted in height so that its apex is placed a common distance above the surface of the block. Variations in the height of a tip (within 0.5 mm) have little effect on the properties of the coating at the tip apex.

Prior to shadowing, the filament is outgassed at a yellow-red heat (approx. 1200K) for 30s at about 6×10^{-6} Torr. The filament temperature is then quickly raised to bright white heat. For a typical filament (0.63mm in diameter and 35mm long), about 12A (at 5V) is required to reach white heat. At this temperature a 2nm layer of tungsten will be deposited onto a tip in ~120s. A commercial quartz crystal deposition monitor is used to check the thickness of the coating during the evaporation process. Good thermal contact between the tungsten tips and the aluminum block insures that the tips will remain close to room temperature during the shadowing process.

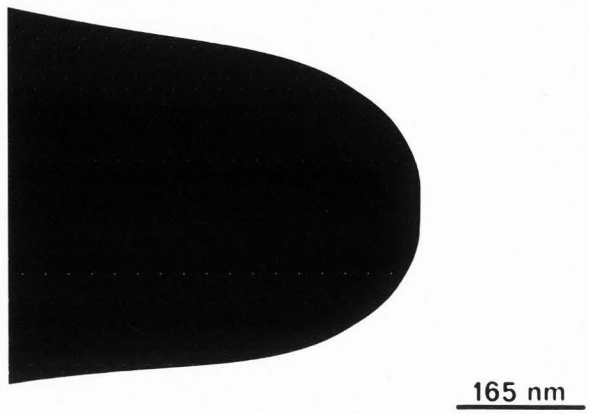

Figure 3. An EPTEM image of a clean tungsten field-emitter tip.

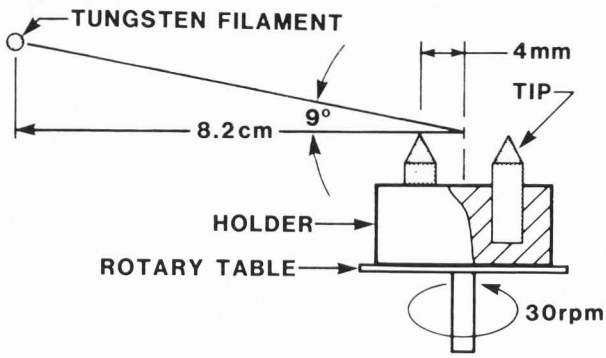

Figure 4. The geometry used to rotary shadow field-emitter tips with metal evaporated from a heated filament.

Substrates that are poor thermal conductors (such as mica) can experience temperature increases of several hundred degrees kelvin during a shadowing procedure (Belous and Wayman, 1967).

Experimental Results

Figure 5a is an EPTEM image taken at 200kV of unshadowed, horse-spleen ferritin molecules. Figures 5b and 5c show the result of rotary shadowing ferritin with a 1nm - 2nm layer of gold, and platinum, respectively. These images were taken at a slight underfocus in order to compare them more directly with images of uncoated ferritin (Figure 5a) used as a control. A slight underfocus is necessary in order to provide adequate contrast to see uncoated ferritin molecules at 200kV.

Ferritin was deposited onto the tips by diffusion, at a concentration of 0.5μg/ml (for two minutes) in a buffer consisting of 50mM HEPES, 150mM NaCl at pH 7.5. After rinsing in buffer, the molecules that adhered to the tip were fixed in a 0.6% solution of glutaraldehyde (in buffer) for five minutes. After fixation, the tips were rinsed in 20%, 50%, and 70% ethanol-water

mixtures, and then rinsed in 100% ethanol and air dried. Deposition and rinsing protocols are described elsewhere in detail (Panitz et al., 1985; Panitz, 1985b).

As expected from numerous examples in the biological literature, gold layers are characterized by closely spaced, individual clusters of gold atoms about 2.5nm in diameter. Platinum layers are similar in appearance, but the clusters are much smaller, typically 1.5nm in size (Figure 6). Platinum layers appear more uniform and more continuous than their gold counterparts. These observations are consistent with sputtering data which suggest that the ratio of the temperature of a metal substrate, T_s, to the melting temperature of the coating material, T_m, determines the morphology of a sputtered layer (Thornton, 1982).

The formation of a continuous metal film on a substrate held at temperature, T_s, is a complicated process that depends upon many parameters including the morphology of the substrate (Thornton, 1982; Chopra, 1969). Metal atoms in the gas phase, produced by some process (e.g. thermal evaporation or sputtering), will collide with a substrate with a kinetic energy kT_m. Depending upon the energy transferred to the substrate during the collision, an incoming atom will lose some (or all) of its kinetic energy. If the remaining kinetic energy (plus the thermal energy acquired from the substrate, kT_s) is greater than the activation energy for surface diffusion, the atom will migrate over the surface (Kellogg et al., 1978). During its random walk, the atom may become trapped, or it may collide with another atom diffusing on the surface. If the activation energy for cluster formation is small, aggregates will form on the surface as a result of these collisions, and the film that grows will be coarse grained and discontinuous. Film continuity can be improved by evaporating at a higher rate (Chopra, 1969). The greater fluence of metal atoms at the substrate surface will cause a higher probability of collision with clusters in their earliest stage of formation. The energy imparted to a cluster during a collision will tend to dissociate the cluster back into its constituent atoms, and the film will be finer grained.

Alternately, film continuity can be improved by reducing the substrate temperature, and by choosing a metal with a high activation energy for surface diffusion and cluster formation. As T_s/T_m decreases, the layer will become finer grained and more continuous (Thornton, 1982). Metal coatings formed on substrates cooled to cryogenic temperatures will have the smoothest structure regardless of the metal used for shadowing. Since condensation of gas phase impurities on the cold surface can degrade film quality, substrate cleaning and evaporation under ultra-high vacuum conditions ($< 10^{-9}$ Torr) is mandatory.

Refractory metals have, in general, the highest activation energies for surface diffusion and cluster formation, at least on metallic substrates (Kellogg et al., 1978). Since tungsten has a much higher melting point than platinum, tungsten will produce a smoother shadow layer that is more useful for high resolution imaging of biological species on room temperature substrates. The effect is well documented (Abermann et al., 1972), and is confirmed by the images in Figure 7.

Figure 7 shows three different biological species rotary shadowed with a thin layer of tungsten. Deposition and rinsing protocols were identical to those previously described for ferritin adsorption. The apparent variation in the diameter of the ferritin molecules seen in Figure 7a highlights a potential difficulty with EPTEM image interpretation. The appearance of a species in a single EPTEM image is related to its position on the highly curved, tip apex. Species that are closer (or further) from the tip apex will be at least partially obscured by the electron opaque, tungsten substrate that is in front (or behind) them. These species can be brought fully into view by rotating the tip about its axis and recording other EPTEM images. A species can be accurately visualized only from a series of EPTEM images obtained as a function of tip rotation, or from a stereo pair (taken at two different tip rotations). The two haemocyanin molecules (from Busycon canaliculatum) shown in Figure 7b have the same apparent size because one molecule is situated directly behind the other. Both molecules are seen because the penetration depth of the 200kV imaging electrons is adequate for complete penetration of both species. The characteristic, rod-like appearance of an enzyme-cleaved, TMV particle (from a sample supplied by P. J. Butler, the MRC, Cambridge, England) is preserved in the EPTEM image of Figure 7c. Figure 8 is an EPTEM image of two TMV particles, each attached to the tip apex by one end. Figure 7c and Figure 8 clearly demonstrate the smooth morphology of a tungsten shadow layer, and its ability to provide high resolution TEM images of biological species.

Summary and Conclusions

Metal layers have been placed onto field-emitter tips coated with biological species by thermal evaporation in high vacuum. The most uniform and continuous coatings were produced by tungsten, evaporated onto tips that were slowly turned about their axis. The proximity of the tips to the incandescent tungsten filament during the evaporation process did not degrade the coating or the appearance of the biological species adsorbed onto the tip surface.

As expected, the continuity and the grain size of the layer that surrounds a biological species on a room temperature substrate is correlated with the melting point of the material used for shadowing. Gold layers exhibit the largest grain size and are discontinuous. Gold melts at 1336K. Platinum layers are finer grained, and more continuous. Platinum melts at 2046K. Tungsten layers are the smoothest and display subnanometer granularity. Tungsten melts at 3643K. The thin tungsten film will readily oxidize in air. Since an oxide layer may produce less contrast in a TEM image than a pure metal, it is worthwhile to consider ways to reduce oxide formation.

Oxidation of the shadow layer can be minimized by rapidly transferring the substrate into the

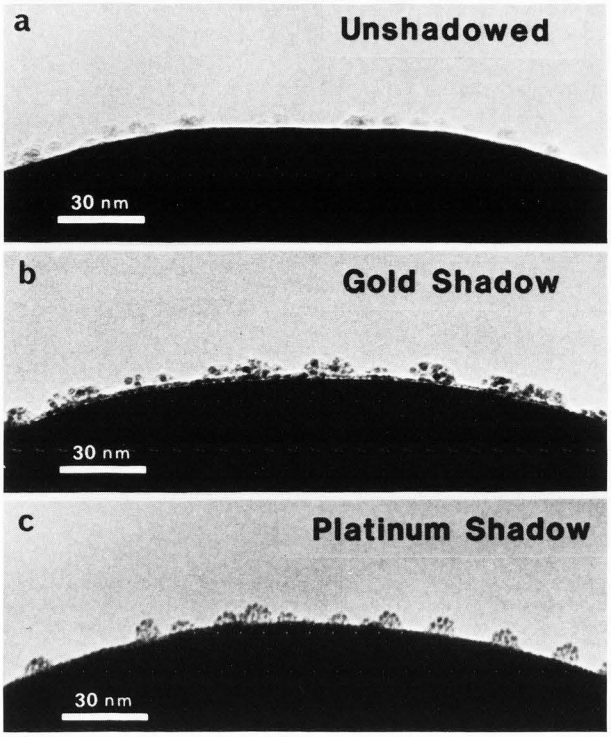

Figure 5. Rotary shadowed horse-spleen ferritin on tungsten field-emitter tips. (a) Unshadowed (control). (b) Gold Shadow. (c) Platinum shadow.

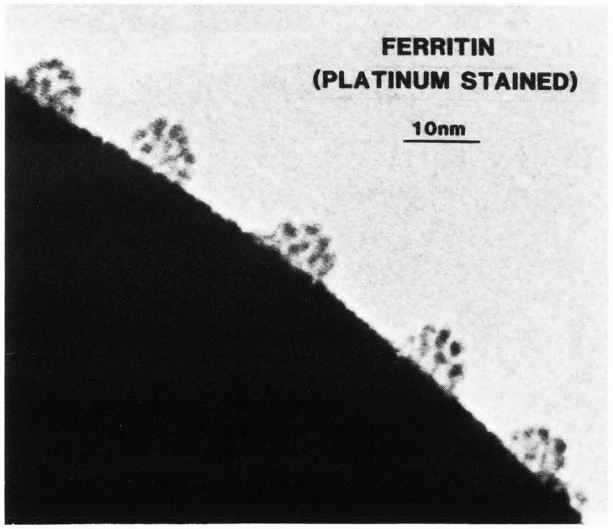

Figure 6. Individual horse-spleen ferritin molecules on a tungsten field-emitter tip, rotary shadowed with platinum.

electron microscope. Oxidation can be further reduced by transferring the substrate in an inert atmosphere of nitrogen or argon. A transfer under high vacuum would eliminate the oxidation problem, but the procedure is complicated, and expensive to implement. Alternately, it is possible to use a

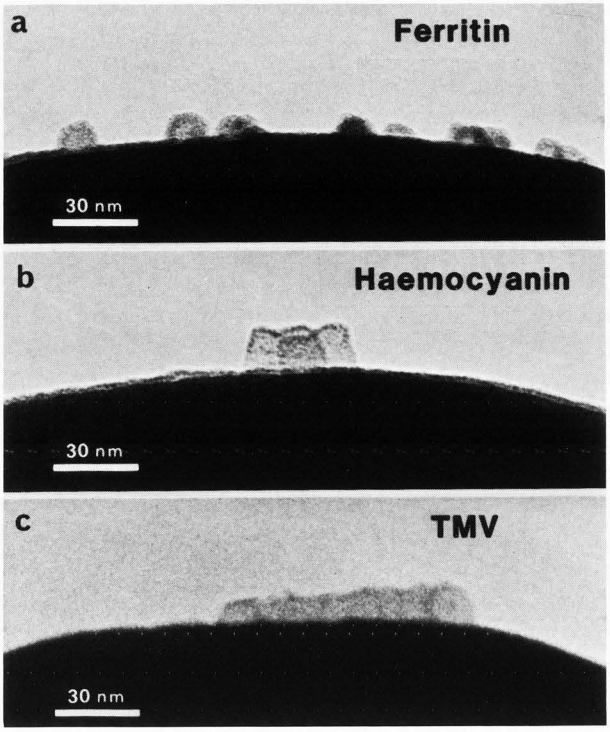

Figure 7. Different biological species on tungsten field-emitter tips, rotary shadowed with tungsten. (a) Horse-spleen ferritin. (b) Haemocyanin (from Busycon canaliculatum). (c) Tobacco mosaic virus (TMV).

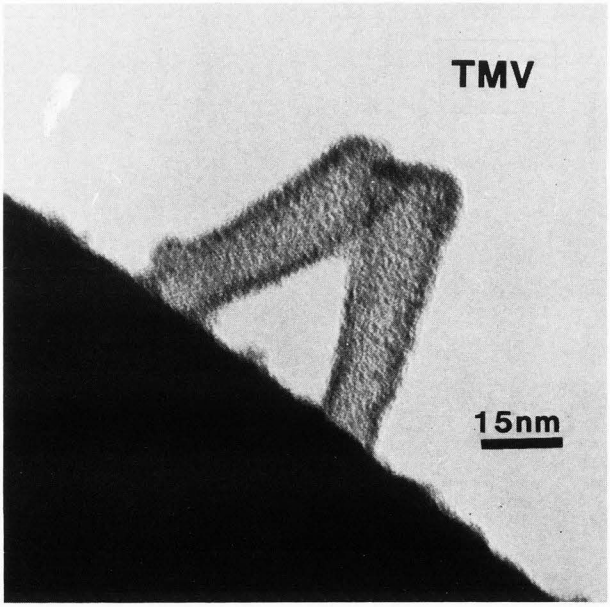

Figure 8. Two tobacco mosaic virus (TMV) particles on a tungsten field-emitter tip, rotary shadowed with tungsten.

less reactive, refractory metal for high resolution shadowing. Iridium and tantalum are two attractive candidates. Both resist oxidation in air, and both metals have a very high melting point. Iridium will produce a finer grained shadow layer than platinum because of its higher melting point (Abermann et al., 1972). Tantalum layers should be even finer grained because of tantalum's higher melting point. Both metals will produce coarser grained layers than tungsten, although tantalum layers may be similar in appearance because of its comparable (but lower) melting point.

Acknowledgement

The author would like to thank the Advanced Biochemical Technology Program at the Defense Advanced Research Projects Agency for supporting this work under ARPA contract # 4597. Tom Headley (SNLA) provided the microscopy support that greatly facilitated this study. David Bear, a molecular biologist in the department of Cell Biology at the University of New Mexico School of Medicine, deserves special thanks for making his laboratory facilities freely available to the author during the course of this investigation. The technical assistance provided by Chris Andrews of his laboratory is gratefully acknowledged.

References

Abermann R, Salpeter MM, Bachmann L. (1972). High Resolution Shadowing, in: Principles and Techniques of Electron Microscopy, M. A. Hayat (ed), Van Nostrand Reinhold, New York, 197-217.

Belous MV, Wayman CM. (1967). Temperature changes in thin metal films during vapor deposition. J. Appl. Phys. 38, 5119-5124.

Boling JL, Dolan WW. (1958). Blunting of tungsten needles by surface diffusion. J. Appl. Phys. 29, 556-559.

Carter FL. (1983). Molecular level fabrication techniques and molecular electronic devices. J. Vac. Sci. Technol. B. 1(4), 959-968.

Chopra KL. (1969). Thin Film Phenomena, McGraw-Hill, New York, 137-265.

Dyke WW, Dolan WW. (1960). Field Emission, in: Advances in Electronics and Electron Physics, L. Marton (ed), Academic Press, New York, 89-185.

Eyring CF, Mackeown SS, Millikan RA. (1928). Field-Electron Emission Current from Points. Phys. Rev. 31, 900-909.

Fisher HW, Williams RC. (1979). Electron microscopic visualization of nucleic acids and of their complexes with proteins. Ann. Rev. Biochem. 48, 649-679.

Griffith JD. (1973). Electron microscopic visualization of DNA in association with cellular components, in: Methods of Cell Biology, D.M. Prescott (ed), Academic Press, New York, 129-146.

Griffith JD, Christiansen G. (1978). Electron microscope visualization of chromatin and other DNA-protein complexes. Ann. Rev. Biophys. Bioeng. B7, 19-35.

Kellogg GL, Tsong TT, Cowan P. (1978). Direct Observation of Surface Diffusion and Atomic Interactions on Metal Surfaces. Surface Sci. 70, 485-519.

Lins N. (1984). Textural image processing of granular structures of metal showing replicas. Ultramicroscopy 12(3) 185-200.

Müller EW. (1937). Elektronenmikroskopische beobachtungen von feldkathoden. Z. Physik 106, 541-550.

Müller EW, Tsong TT. (1969). Field-Ion Microscopy: Principles and Applications, Elsevier, New York, 119-127.

Müller M, Downing KH, Kubler O, Koller T. (1975). Encapsulation of macromolecules into "low noise" supports. J. Microscopie (Paris) 23, 117-125.

Panitz JA. (1985a). Biomolecular Adsorption and the LIFE detector. in: Proceedings of the 31st International Field-Emission Symposium, P. Sudraud (ed), J. de Physique. 45(12/C9), 285-291.

Panitz JA. (1985b). Biomolecular deposition on multiple field-emitter tips. Rev. Sci. Instrum. 56(4), 572-574.

Panitz JA, Bear DG. (1985) A procedure for increasing the contrast of biological specimens in edge-projection TEM. J. Microscopy (Oxford) 138, 107-110.

Panitz JA, Andrews CL, Bear DG. (1985). A deposition technique for the imaging and analysis of protein interactions with metal and semiconductor surfaces. J. Electron Microscopy Techniques 2, 285-292.

Panitz JA, Giaever I. (1980). Protein deposition on field- emitter tips and its removal by UV radiation. Surf. Sci. 97, 25-42.

Panitz JA, Giaever I. (1981). Ferritin deposition on field- emitter tips. Ultramicroscopy 6, 3-6.

Thornton JA. (1982). Coating deposition by sputtering, in: Deposition Technologies for Films and Coatings, R. F. Bunshah (ed), Noyes Publications, Park Ridge, NJ, 170-243.